

Original Research

Cytotoxic capacity of a novel glycosylated antitumor ether lipid in chemotherapy-resistant high grade serous ovarian cancer *in vitro* and *in vivo*

Mark W Nachtigal^{a,b,c,*}, Paris Musaphir^a, Shiv Dhiman^d, Alon D Altman^b, Frank Schweizer^d, Gilbert Arthur^a

^a Department of Biochemistry and Medical Genetics, University of Manitoba, 301 BMSB-745 Bannatyne Avenue, Winnipeg, Manitoba R3E 0J9, Canada

^b Department of Obstetrics, Gynecology and Reproductive Sciences, University of Manitoba, Winnipeg, Manitoba R3E 0J9, Canada

^c CancerCare Manitoba Research Institute, Winnipeg, Manitoba R2H 2A6, Canada

^d Department of Chemistry, University of Manitoba, Winnipeg, Manitoba R3T 2N2, Canada



ARTICLE INFO

Keywords:

Glycosylated antitumor ether lipid (GAEL)
Ovarian cancer patient sample
3d spheroid
Chicken chorioallantoic membrane (cam) model
OVCAR3 xenograft

ABSTRACT

Chemotherapy resistant high grade serous ovarian cancer remains a clinically intractable disease with a high rate of mortality. We tested a novel glycosylated antitumor ether lipid called L-Rham to assess the *in vitro* and *in vivo* efficacy on high grade serous ovarian cancer cell lines and patient samples. L-Rham effectively kills high grade serous ovarian cancer cells grown as 2D or 3D cultures in a dose and time dependent manner. L-Rham efficacy was tested *in vivo* in a chicken allantoic membrane/COV362 xenograft model, where L-Rham activity was as effective as paclitaxel in reducing tumor weight and metastasis. The efficacy of L-Rham to reduce OVCAR3 tumor xenografts in NRG mice was assessed in low and high tumor burden models. L-Rham effectively reduced tumor formation in the low tumor burden group, and blocked ascites formation in low and high tumor burden animals. L-Rham demonstrates efficacy against OVCAR3 tumor and ascites formation *in vivo* in NRG mice, laying the foundation for further development of this drug class for the treatment of high grade serous ovarian cancer patients.

Introduction

Chemotherapy resistant disease remains the primary cause of patient mortality and morbidity among human epithelial ovarian cancer (EOC)¹ patients. High-grade serous ovarian cancer (HGSOC) accounts for 70% of all EOCs [1], and is the most lethal histological subtype [2,3]. While initially responsive to the apoptosis-inducing drugs used as standard of care, carboplatin and paclitaxel, 75% of HGSOC patients will relapse within 18 months. Although additional lines of chemotherapeutics are routinely used, these treatments ultimately fail [2]. As such, there is a clinical demand for novel therapeutics capable of killing chemoresistant EOC cells. We developed compounds called Glycosylated Antitumor Ether Lipids (GAELs) that kill numerous human cancer cell types through an apoptosis-independent mechanism [4–8]. Furthermore, we

determined that chemotherapy-resistant EOC cells are exquisitely sensitive to these drugs [5], suggesting that they can bypass the mechanisms HGSOC cells use to evade carboplatin- and paclitaxel-induced cell death. We propose that GAELs may be developed as a new drug class to reduce the burden of cancer for HGSOC patients [5,9].

GAELs are a subclass of antitumor ether lipids (AEL) and are distinguished by the presence of an anomeric sugar moiety in the molecule. The prototypic AEL 1-O-Octadecyl-2-O-methyl-rac-glycero-phosphocholine (ET-18-OCH3) [10], a representative of the alkylsophospholipid subclass, showed promise in clinical trials, but was ultimately not widely embraced as a novel chemotherapy for treating human cancer [11–13]. This is most likely due to the susceptibility of AELs to anti-apoptotic mechanisms utilized by cancer cells. Our initial studies with GAELs, primarily with D sugar analogues [4–9,14,15] also

* Corresponding author at: Department of Biochemistry and Medical Genetics, University of Manitoba, 301 BMSB-745 Bannatyne Avenue, Winnipeg, MB R3E 0J9, Canada.

E-mail address: mark.nachtigal@umanitoba.ca (M.W. Nachtigal).

¹ antitumor ether lipids (AEL); BC Cancer Agency Investigational Drug program (BCCA-ID); chicken allantoic membrane (CAM); cytotoxic concentration to cause death to 50% of viable cells (IC₅₀); chromosome instability (CIN); dose range finding (DRF); epithelial ovarian cancer (EOC); Glycosylated Antitumor Ether Lipids (GAELs); high grade serous ovarian cancer (HGSOC); maximum tolerated dose (MTD); NOD-Rag1^{null} IL2rg^{null} (NRG); 3-amino-1-O-hexadecyloxy-2R-(O-α-L-Rhamnopyranosyl)-sn-glycerol (L-Rham); Q-VD-OPh (Q-VD)

<https://doi.org/10.1016/j.tranon.2021.101203>

Received 10 August 2021; Accepted 11 August 2021

1936-5233/© 2021 Published by Elsevier Inc. This is an open access article under the CC BY-NC-ND license (<http://creativecommons.org/licenses/by-nc-nd/4.0/>).

showed great promise in their ability to kill a wide range of human cancer cell lines, but a lack of activity *in vivo* hampered their development as treatment agents [16]. Metabolic inactivation was likely due to glycosidase cleavage of the carbohydrate moiety, a problem shared by many carbohydrate-based molecules [17,18]. Our previous structure/activity studies that aimed to improve the activity and metabolic stability of GAELs led to the development of two distinct types of L-GAELs distinguished by the position of critical amino moiety in the molecule that is required for activity. One type has the sugar attached to the C-3 position of the glycerol backbone with the amine attached at the C-2 position of the sugar [19], while the other has the sugar attached at the C-2 position of glycerol and the amine attached to the C-3 position of the glycerol [20]. The L-sugar-linked GAEL analogues [20] are not susceptible to circulating and cellular glycosidases *in vivo*, and are likely to retain the sugar linkage that is essential for activity, and potentially have high efficacy *in vivo*.

The current investigation focused on evaluating the effects of a recently developed GAEL, 3-amino-1-*O*-hexadecyloxy-2R-(*O*- α -L-Rhamnopyranosyl)-*sn*-glycerol (L-Rham; Fig. S1)[20] on chemo-naïve, chemosensitive and chemoresistant HGSOC cell lines and primary samples derived from HGSOC patient ascites. Activity of L-Rham was tested using HGSOC cells grown as 2-dimensional (2D) adherent monolayers and as 3D spheroids or aggregates [5,21]. These *in vitro* studies were complemented by testing L-Rham tolerability and efficacy *in vivo* using chicken chorioallantoic membrane (CAM) COV362 xenograft and murine OVCAR3 xenograft models. This research demonstrates L-Rham efficacy to reduce the burden of HGSOC *in vivo* and provides a foundation to develop this class of drugs further for the treatment of HGSOC patients.

Materials and methods

Ethics approval statement for human samples

This study included the collection and use of HGSOC ascites-derived patient samples after receiving patient consent (University of Manitoba Research Ethics Board, #HS19242).

Cell culture

All cell lines and primary HGSOC cell samples were maintained at 37 °C with 5% CO₂/95% air, and grown as previously described [5,21]. The CaOV3 (RRID:CVCL_0201) and OVCAR3 (RRID:CVCL_0465) cell lines were cultured from frozen stocks obtained from the ATCC (Manassas, VA, USA); TOV1946 (RRID:CVCL_4062) were received from the OVCAN collection; COV362 (RRID:CVCL_2420) were purchased from SIGMA and frozen stocks made after first passage. All experiments were conducted with cells thawed from frozen stocks. Known characteristics of the HGSOC patient samples are listed in Table S1. Regarding sample nomenclature, cells isolated from serial paracentesis samples of the same patient have the same number followed by a letter (e.g., EOC 183E, EOC 183I, EOC 183J). Letters may not be contiguous due to samples used for other research projects or failure of the sample to grow in culture.

Drugs

3-amino-1-*O*-hexadecyloxy-2R-(*O*- α -L-Rhamnopyranosyl)-*sn*-glycerol (L-Rham) was synthesized as described in Ogunsin et al. [20]. L-Rham stocks for *in vitro* experiments were heated to 60 °C in a water bath to solubilize the lipids prior to dilution in growth medium or 0.9% saline for addition to the cells or mice. Carboplatin (Tocris Bioscience) was reconstituted in sterile water. Sterile water or 0.9% saline was used as vehicle controls where applicable.

Determination of cytotoxicity of L-Rham on HGSOC cells

The effects of the GAELs on the viability of the HGSOC cell lines and primary cell samples grown as adherent monolayers or as non-adherent aggregates or spheroids were determined as previously described [5,6,19,20]. Briefly, equal numbers of the cells were dispersed into six wells for each condition into 96-well plates, with 2 wells per condition without cells used as a blank for the fluorescent viability assay. After 24 h for adherent cultures or 48 h for non-adherent cultures, the wells were incubated with the compounds (0–30 μ M) for specified times. Following incubation with drug, cell viability was measured using PrestoBlue Cell Viability reagent (Invitrogen) according to manufacturer's protocol and fluorescence (540/590 nm) measured with a plate reader (Molecular Probes). Values from the wells without cells (blank wells) were subtracted from the corresponding sample wells and cell viability was compared relative to the vehicle control samples set to 100%. Thus, relative cell viability of 0% indicates that there are no viable cells. Relative fluorescence units were input into Prism9 for statistical analysis and generation of graphs. The results represent the mean \pm standard deviation of a minimum of 3 independent experiments with 6 samples per experiment.

To measure caspase-dependent cell death, cells were plated in 96-well plates and allowed to adhere overnight prior to drug treatment. Cells were pre-treated for 1 h with the pan-caspase inhibitor Q-VD-OPH (Q-VD; 10 μ M; MedChem Express) followed by addition of L-Rham or carboplatin without or with the inhibitor for an additional 48 h (or 72 h for carboplatin). Cell viability was determined using PrestoBlue Cell Viability reagent as outlined above. Wells with media but no cells were treated in similar fashion and the values utilized as blank.

Chorioallantoic membrane (CAM)/COV362 xenograft assay and drug toxicity

Experiments with chick embryos comply has been recognized as an alternative to mouse xenografts for *in vivo* experiments by the National center for the Replacement, Refinement and Reduction of Animals in Research (NC3R, UK) and all experiments complied with European Directive 2010/63/EU. The efficacy and toxicity of L-Rham on COV362-derived tumors in a chicken CAM xenograft model was independently assessed by INOVOTION SAS, France (www.inovotion.com) on a fee-for-service basis. Fertilized White Leghorn eggs are incubated at 37.5 °C with 50% relative humidity for 9 days. At this time (E9), the chorioallantoic membrane (CAM) was dropped by drilling a small hole through the eggshell into the air sac, and a 1 cm² window was cut in the eggshell above the CAM. An inoculum of 3 \times 10⁶ COV362 cells was added onto the CAM of each egg. Twenty-one eggs were used for each condition (because of some early egg deaths, just after grafting or some bad tumor grafts, data was collected in less than 21 eggs per group). Eggs were then randomized into 4 groups. Group 1 = Vehicle (0.9% saline); Group 2 = 50 μ M paclitaxel; Group 3 = 200 μ M L-Rham; Group 4 = 400 μ M L-Rham. At day 10 (E10), COV362 tumors began to be detectable. They were then treated for the next 8 days. Every two days (E11, E13, E15, E17) tumors were treated by placing 100 μ l of vehicle or drug onto the tumor. At day 18 (E18) the upper portion of the CAM was removed, washed in PBS and then directly transferred in paraformaldehyde and fixed for 48 h. The tumors were then carefully cut away from normal CAM tissue and weighed. A one-way ANOVA analysis with post-hoc tests was done to assess if the drug treatments had an effect compared to vehicle.

In parallel, a 1 cm² portion of the lower CAM was collected from half of the available samples to evaluate the number of metastasis cells. Genomic DNA was extracted from the CAM, and analyzed by qPCR with specific primers for human Alu sequences. Statistical analysis was directly done on data from the Bio-Rad CFX Manager 3.1 software.

Drug toxicity was determined by measuring the number of embryos alive at the end of the treatment period and identifying any visible macroscopic abnormalities in the embryos.

Drug tolerability studies in mice

In vivo drug tolerability studies were conducted by the BC Cancer Agency Investigational Drug program (BCCA-ID). Animals were maintained according to the Canadian Council on Animal Care, and institutional ethical approval for research with animals was received prior to

the initiation of these studies (University of British Columbia, A18-0290). All animals were maintained in a temperature-controlled environment at 22 °C on a 12 h light:12 h darkness schedule and provided with food and tap water *ad libitum*. The acute response, tip-toe gait, lethargy, piloerection and respiration in addition to body weight measurements were recorded to assess negative drug effects. 6–8-week-old

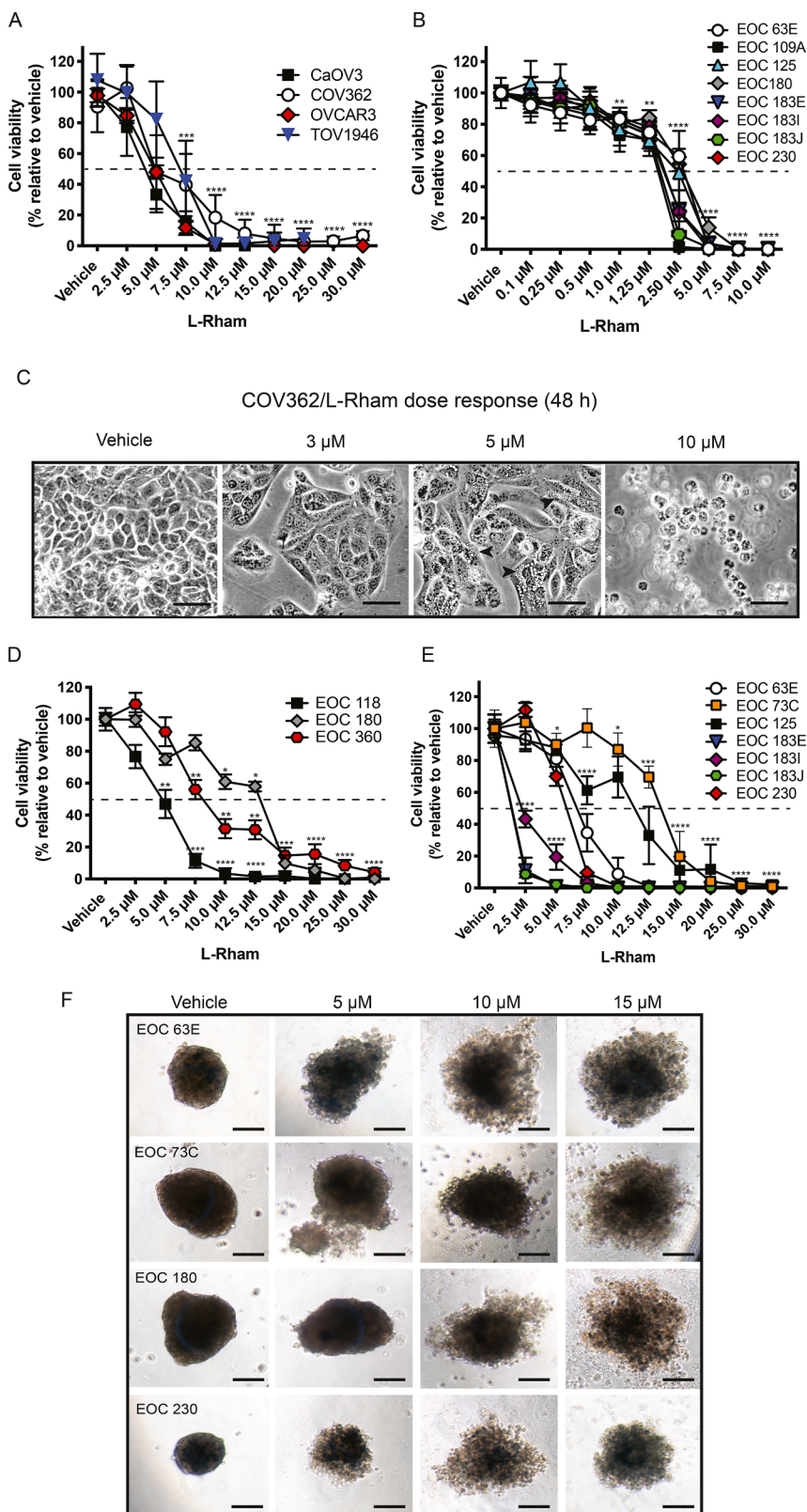


Fig. 1. HGSOC cell viability after L-Rham treatment. **A.** Dose response of established HGSOC cell lines treated with L-Rham for 48 h. Cells were grown as adherent monolayers. For A, B and C cells were grown as adherent monolayers, and for D, E and F cells were grown as non-adherent cell aggregates or spheres (depending on the individual sample). The dashed lines indicate 50% cell viability. Asterisks (*) indicate significant difference from vehicle treated cells. **B.** Dose response of chemosensitive and chemoresistant HGSOC patient samples treated with L-Rham for 48 h. **C.** COV362 morphologic response to increasing doses of L-Rham at 48 h. Note vesicle formation (arrowheads) at 5 μM L-Rham. **D, E.** Dose response of chemosensitive HGSOC patient samples treated with L-Rham for 48 h. **F.** Alteration in spheroid morphology in response to increasing doses of L-Rham at 48 h. Solid bar = 100 μm.

female NOD-Rag1^{null} IL2rg^{null} (NRG) mice (3 per condition) were used. Mice received drug by intraperitoneal (i.p.; 15–40 mg/kg) or intravenous (i.v.; 1–50 mg/kg) injection on M/W/Fx2 or every 4 days for 4 injections (Q4Dx4), and then clinically monitored for an additional 14 days. Animal health was monitored and necropsy was performed after termination. Body weight was quantified as an indirect measure of general health.

In vivo drug efficacy studies in mice

Xenograft studies were conducted through the BCCA-ID. 6–8 week old female NRG mice (six per condition) were injected i.p. with 10×10^6 OVCAR3 cells in 200 μ L and drug treatments were initiated 7 days (low tumor burden) or 40 days (high tumor burden) post OVCAR3 cell injection (Q4Dx8). Animals were terminated due to ill-health, tumor progression, or reaching the pre-determined study endpoint. Necropsy was conducted and the presence of ascites and tumor(s) within the peritoneal cavity was noted.

Results

Measuring sensitivity of HGSOc cells to L-Rham

The ability of L-Rham to affect cell viability was assessed using different HGSOc cell lines (CaOV3, COV362, OVCAR3, TOV1946) and primary HGSOc cell samples ($N = 11$) isolated from patients that were chemo-naïve, chemosensitive, or chemoresistant (Table S1). Chemoresistance is defined as responding to platinum drugs for less than 6 months, or as disease progression following the last line of chemotherapy. HGSOc cells were grown as 2D or 3D cultures. The inhibitory concentration to inhibit viable cell numbers to 50% (IC₅₀) for the established HGSOc cell lines grown as 2D cultures ranged from ~4.2–7.1 μ M after 48 h of treatment (Fig. 1A). L-Rham concentrations of 10 μ M were sufficient to kill all the cell lines with the exception of COV362 which required 12.5 μ M to eliminate all the cells.

HGSOc patient cell samples grown as 2D cultures showed similar responses to each other (Fig. 1B); however, they were more sensitive than the established HGSOc cell lines with IC₅₀ ranging from ~1.6–2.8 μ M. Complete cell death was observed at 5 μ M for all the patient samples except EOC180 which required a concentration of 7.5 μ M to eliminate all the cells. The morphological response to L-Rham was similar in cell lines such as COV362 (Fig. 1C) or primary patient samples (Fig. S2).

To gain insight into how L-Rham may affect cells growing in non-adherent (3D) cultures where the cells form large aggregates or spheroids, similar to those shown in Moraya et al. [5], HGSOc patient samples were plated in ultra-low attachment plates. After 48 h, aggregates/spheres were treated with increasing doses of L-Rham for 48 h. Samples that were chemo-naïve or chemosensitive (Fig. 1D) exhibited a range of sensitivity (IC₅₀ = 4.8–13 μ M). Concentrations required to kill all the cells ranged from 10 μ M for EOC 118, 20 μ M for EOC 180 and 30 μ M for EOC 360. Similarly, a range of sensitivity was observed for samples obtained from patients clinically defined as chemoresistant (IC₅₀ range, 1.4–13.8; Fig. 1E). While some samples showed similar sensitivity when grown as adherent or non-adherent cultures (EOC 183E, EOC 183I, EOC 183 J) others showed a difference in their sensitivity (EOC 180A, EOC 230). For example, the IC₅₀ for chemo-naïve EOC 180A as a 2D culture was ~2.7 μ M, but was ~13 μ M when grown as a 3D spheroid. This is not unexpected since cells grown as non-adherent cultures typically exhibit a higher threshold to the cell killing effects of chemotherapeutic drugs [5]. Concentrations required to kill the cells after 48 h incubation ranged from 5 to 20 μ M depending on the cell sample. It is worth noting that L-Rham was capable of killing all the cells regardless of their chemosensitivity.

After 48 h, loss of sphere integrity in the L-Rham treated samples was evident compared to vehicle treated samples (Fig. 1F). At 5 μ M L-Rham,

cells on the periphery of the sphere dissociate and the spheres appear less compacted. Greater loss of sphere compaction is apparent with increasing dose of L-Rham. Loss of sphere compaction correlates with the decreased cell viability (Fig. 1D and E), similar to what we previously observed when breast cancer (BT-474) or prostate cancer (Du-145) stem cell-derived spheroid were treated with different GAEL compounds [6]. These results clearly show that L-Rham is capable of causing the cell death *in vitro* of HGSOc cells obtained from patients clinically defined as chemo-naïve, chemosensitive, or chemoresistant.

Previous research from our laboratories showed that GAELs induce cell death that is not dependent on the caspase cascade [4,5,7]. To determine if this was also characteristic of L-Rham cytotoxicity on HGSOc cells, the CaOV3, COV362, and OVCAR3 cell lines were treated with increasing doses of L-Rham in the absence or presence of the pan caspase inhibitor Q-VD-OPH (Q-VD; 10 μ M). Similar to our previous results [5], the presence of Q-VD did not alter the degree of cell death induced by L-Rham, but Q-VD efficiently inhibited caspase-dependent cell death induced by carboplatin (Fig. S3).

Temporal sensitivity of HGSOc cells to L-Rham

Our previous work demonstrated effective cell killing of human breast cancer (BT-474) or prostate cancer (DU-145) cell spheroids over time [6]. To evaluate a temporal effect on HGSOc patient samples, we initially examined the cell killing effect of L-Rham on chemo-naïve (EOC 16B, EOC 58) and chemoresistant (EOC 16H) HGSOc patient samples for 96 h. The IC₅₀ ranged between 1 and 1.75 μ M (Table 1), with the chemoresistant sample (EOC 16H) showing the greatest sensitivity. Analysis of an additional chemo-naïve (EOC 180; Fig. 2A) and chemoresistant (EOC 73C; Fig. 2B) sample grown as spheroids showed a consistent leftward shift in sensitivity over time (up to 96 h) after a single drug treatment at 0 h. Specifically, the IC₅₀ for EOC 180 changed from 13.4 μ M at 48 h to 8.7 μ M at 96 h. Similarly, the IC₅₀ for EOC 73C changed from 14.3 μ M at 48 h to 7.8 μ M at 72 h. The concentration of L-Rham required to kill all the cells also decreased with increasing time of incubation. These results demonstrate that treatment with L-Rham is effective over time on chemo-naïve and chemoresistant HGSOc patient samples.

Effect of L-Rham on a chorioallantoic membrane (CAM)/COV362 xenograft

While we demonstrated the ability of GAELs to kill a wide variety of human cancer cells *in vitro* [4–9,15,19,20,22], our next step was to test the efficacy of a GAEL in an *in vivo* system using L-Rham as a model GAEL. The efficacy and toxicity of L-Rham on COV362-derived tumors was tested in a chicken CAM xenograft model (experimental timeline shown in Fig. 3A). Due to the potential of reagents to diffuse throughout the entire egg, high drug concentrations are used. Given the volume of an egg, 200 μ M and 400 μ M of L-Rham diffused throughout the egg would be roughly equal to 0.44 and 0.88 μ M *in ovo*, respectively. Paclitaxel (50 μ M; 0.11 μ M *in ovo*) was used as a positive cell killing agent for comparative purposes. Compared to vehicle treated COV362

Table 1

Percent viability of primary EOC cells grown as 3D spheroids after treatment with increasing concentrations of L-Rham over 96 h.

(μ M L-Rham)	EOC 16B	EOC 16H	EOC 58
Vehicle	100	100	100
0.25	84.9 \pm 15.04	78.22 \pm 7.91	99.18 \pm 8.68
0.5	62.67 \pm 6.19	73.15 \pm 9.49	105.36 \pm 0.93
1.0	74.18 \pm 0.12	50.85 \pm 9.3	81.55 \pm 7.5
1.5	18.95 \pm 9.89	22.92 \pm 9.13	60.36 \pm 6.37
2.0	7.53 \pm 6.17	5.89 \pm 3.36	20.16 \pm 8.19
3.0	8.43 \pm 0.91	6.41 \pm 2.01	8.36 \pm 8.26
4.0	9.10 \pm 4.38	–	4.71 \pm 2.17

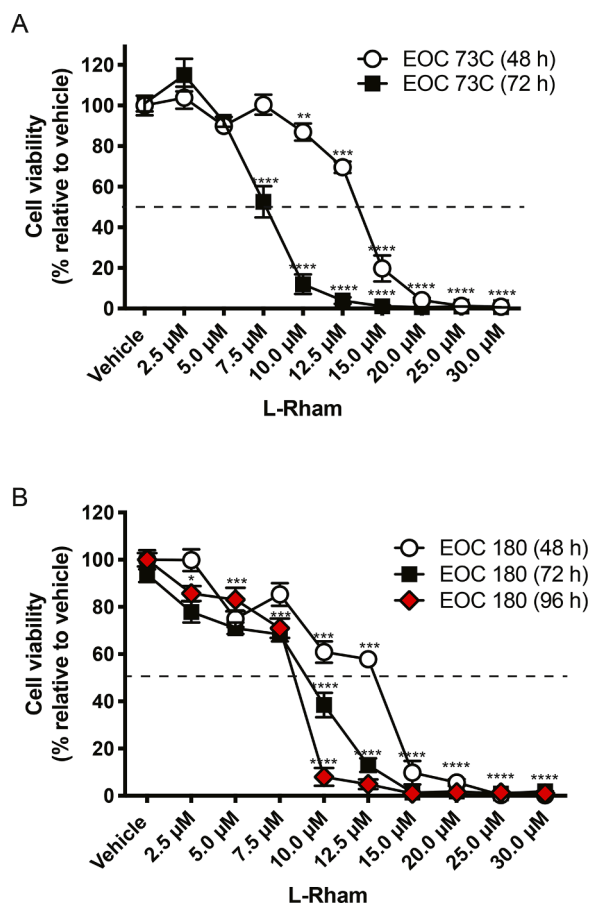


Fig. 2. HGSOC patient sample viability in response to L-Rham over time. **A, B.** Time course of HGSOC patient samples (EOC 73C and EOC 180) treated with increasing doses of L-Rham (single treatment at time = 0 h). Cells were grown as non-adherent (3D) tumorspheres. Note the leftward shift in sensitivity over time. The dashed lines indicate 50% cell viability. Asterisks (*) indicate significant difference from vehicle treated cells.

tumors, tumor weight was reduced by treatment with L-Rham (14–18%) to the same extent as paclitaxel-treated tumors (15% reduction; Fig. 3B and Table S2). Similarly, the extent of COV362 metastasis through the CAM showed L-Rham had the same efficacy as paclitaxel in reducing metastasis of COV362 cells (Fig. 3C and Table S3).

Analysis of potential toxicity showed a similar level of embryo survival for all groups averaging 86.5%, with the 200 μM L-Rham group having the highest survival at 93% compared to the vehicle group (83%) (Table S4). Moreover, there were no visible abnormalities of any drug-treated embryos, which included assessment of head formation, body development, limb evolution, skin, and extraembryonic tissue. While this model is excellent for drug screening purposes, a limitation of this model is that drug treatment was available to a maximum of 8 days and may not reveal the full effect(s) of a test compound, nor did it account for mammalian metabolism.

L-Rham dose range finding (DRF) and maximum tolerated dose (MTD) in a murine model

To evaluate L-Rham drug tolerability in a mammalian model, the BCCA-ID was contracted to conduct DRF and MTD studies in immunocompromised NRG mice. I.v. and i.p. delivery was tested using two vehicles, 1% propylene glycol (PG) and 0.9% saline, and different drug delivery schedules (Fig. 4A). Mice administered L-Rham in PG i.v. were observed to display signs of pain and swelling at the injection site, so all i.v. delivery studies were discontinued. The MTD for L-Rham in NRG

mice when administered i.p. was 20 mg/kg with 1% PG (MWFx2) or 15 mg/kg with 0.9% saline (Q4Dx4). Mild clinical signs of toxicity were observed, but these resolved prior to necropsy. Drug treatment that was tested, but not tolerated, included multiple doses of L-Rham delivered i.p. at 40 mg/kg in 1% PG (MWFx2) that caused abdominal tenseness and distension, body weight loss, pain, coat piloerection, pale extremities and dehydration. A detailed description of the necropsy results following drug administration for the MTD studies is provided (Table S5). Thus, L-Rham showed tolerable toxicity at orders of magnitude higher than those that kill primary HGSOC cell spheroids *in vitro* and suggested that L-Rham may be well tolerated at therapeutic doses.

Measuring L-Rham efficacy in an OVCAR3 murine xenograft model

As an initial step toward conducting *in vivo* efficacy studies, an OVCAR3 i.p. xenograft model in female NRG mice was developed with the BCCA-ID. This cell line was selected because of the wealth of data indicating the ability to OVCAR3 cells to form solid tumors *in vivo* after i.p. injection of cells [23]. Mice (6 per condition) were monitored for up to 100 days after OVCAR3 cell injection. By day 52–56 all mice showed mild abdominal distension, with moderate distension lasting between day 56 and 79, followed by the most severe abdominal distension. At day 99 three mice were euthanized due to morbidity, and the other three were terminated at the end of study (day 100). All mice had approximately 5 ml of ascites and numerous i.p. tumors (1–6 mm³) dispersed throughout the peritoneal cavity (e.g., uterine horns, spleen, and liver) similar to previously published data [23].

The ability of L-Rham to modify tumor growth was examined in NRG mice with OVCAR3 i.p. xenografts in an end-point study as opposed to a survival study. Models of treatment where mice had low or high tumor burden at the time of drug treatment were tested (Table S6; 6 mice per condition; NB. Group 2 had 12 mice) for a set period of time. The longest the xenografts were allowed to grow for the efficacy studies was 74 days. This decision was made to balance the ability to assess drug efficacy with the comfort of the animals. To evaluate efficacy, vehicle or L-Rham (15 mg/kg in 0.9% saline, i.p., Q4Dx8) treatment was initiated 7 days after OVCAR3 cell injection i.p. (low tumor burden) or starting 41 days after OVCAR3 injection (high tumor burden). One group of low tumor burden animals was terminated at day 41 (Groups 1 and 3), while another low tumor burden cohort (Group 4) and the high tumor burden cohort (Groups 2 and 5) were terminated 74 days after OVCAR3 cell injection.

For the cohorts terminated at day 41 after cell injection, only 1 of the 6 (17%) Group 1 (Vehicle) mice had a measurable tumor on the abdominal wall (5 mm³), while all the mice had enlarged inguinal lymph nodes (Table 2 and Fig. 4B). No tumors (0%) were detected in the Group 3 (L-Rham treated) mice. Most of the L-Rham treated mice exhibited moderate generalized peritonitis causing adhesions of the ovary, bladder, intestines, liver, kidney, stomach, uterus to the peritoneal wall, an apparent side-effect of the L-Rham delivery schedule. Details of the tumor burden and necropsy findings for each mouse are shown in Tables S7 and S8, respectively.

For cohorts designed to be terminated on day 74, 12 of 12 (100%) Group 2 mice (Vehicle) had tumors on the peritoneal organs ranging in size from 0.5 to 6 mm³ (Fig. 4B), and 11 of 12 (92%) mice had detectable ascites, but only 4/12 (33%) had ascites in measurable volumes (range: 75–200 μL; Tables 2, S7 and S8, and Fig. 4C). By contrast, only 2 of 6 (33%) Group 4 mice (L-Rham treated, low tumor burden) exhibited peritoneal tumors (Fig. 4B); 1 mouse had one 5 mm³ tumor on the pancreas, and one mouse had multiple <1mm³ tumors on the liver. None (0%) of the Group 4 mice had detectable ascites (Fig. 4C). For the Group 5 mice (L-Rham treated, high tumor burden), all animals (100%) exhibited numerous tumors (0.5–8 mm³) on the peritoneal organs, but no ascites was detected (Fig. 4B and C; Tables 2, S7 and S8). There were no statistically significant differences in the mean tumor mass between Groups 2, 4, and 5 (Kruskal-Wallis, $P = 0.7265$). Similar to Group 3, all

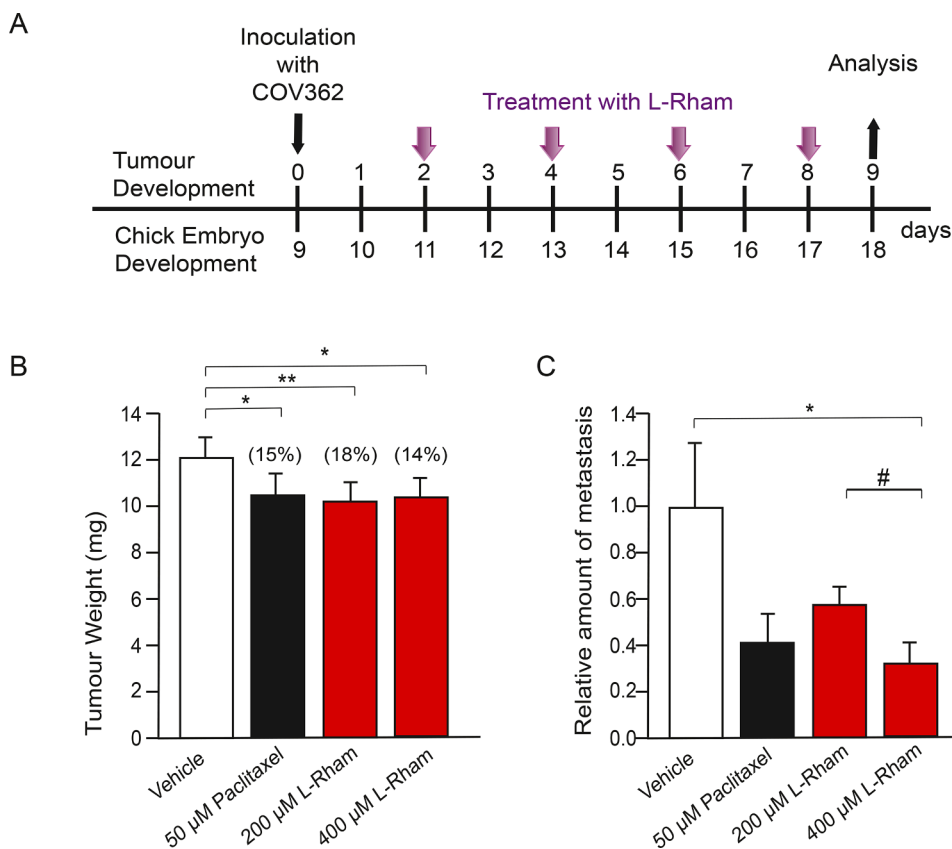


Fig. 3. Chicken embryo chorioallantoic membrane assay to examine the effect of L-Rham on COV362 cell xenograft model. A. Experimental time course showing time of COV362 cell injection and L-Rham (200 or 400 µM) treatments. 50 µM Paclitaxel was used as a positive control. At the study termination, viability of embryos was the same in all groups (~90%). **B.** Tumor weight was significantly reduced for each group (14–18%). **C.** Metastasis relative to vehicle control showed a significant effect (*) for the highest dose of L-Rham. A significant difference (#) was observed between 200 µM and 400 µM L-Rham ($N = 18$ eggs per group).

mice in Groups 4 and 5 showed some degree of peritonitis (Tables 2 and S8). These results show that L-Rham is effective at treating animals with a low tumor burden, and are capable of eliminating ascites formation in all animals, even those with a high tumor burden.

Discussion

There is a clinical need to identify novel drugs or treatment regimens to reduce tumor burden in chemotherapy-resistant HGSOC patients. We demonstrate that L-Rham is a novel GAEL capable of killing HGSOC cell lines and primary cells isolated from patient ascites (regardless of chemotherapy sensitivity status) *in vitro* when grown as 2D or 3D cultures. A significant take away message from the *in vitro* studies was that L-Rham is able to completely eliminate all viable cells from the 2D or 3D cultures. This ability to completely eradicate viable cells would be useful in minimizing the problem of residual cells that could potentially regenerate the tumor. Importantly, we show for the first time that a GAEL, L-Rham, can reduce tumor burden *in vivo* in two models. Specifically, the CAM model demonstrated a reduction in tumor mass and metastatic potential equivalent to paclitaxel. In a murine xenograft model, L-Rham reduced or prevented tumors growing in the low tumor burden group and prevented ascites formation in all treated groups. These results lay the foundation for further development of GAELs as a potential novel drug class that may be used for the treatment of patients with chemotherapy resistant HGSOC.

GAELs possess many desirable anticancer characteristics that include: (1) killing chemoresistant cell lines and primary HGSOC cells grown as 2D or 3D cultures and cause the disaggregation of 3D spheroids [5–7,19]; (2) killing human cancer stem cell-enriched fractions from breast and prostate cell lines [6,8,19]; and (3) killing cells via an apoptosis-independent mechanism of action [4–8]. This latter characteristic distinguishes GAELs from most of the currently used chemotherapeutic drugs that rely on apoptosis to kill HGSOC cells. While the

molecular mechanism of action of GAELs is not completely known, we have established that GAELs do not kill cells via autophagy or a caspase-dependent mechanism [4,5,7]. We previously reported that after cells were incubated with the prototypical GAEL called GLN, cathepsins B, D, and L were released into the cytosol and an increase in cathepsin activity was detected [4]. Furthermore, in cells pretreated with pepstatin A, an inhibitor to cathepsin B, cell death was partially inhibited in response to GLN. A more limited study in EOC cells (encompassing HGSOC and clear cell histotypes) revealed that pepstatin A did partially attenuate GLN-induced cell death in some primary EOC cells but not in others [5]. We have also shown that alteration of mitochondrial membrane potential, which is essential for paraptosis or oncosis, two non-apoptotic death pathways [7], does not occur in GAEL-treated cells [7]. GAEL-induced cell death is intimately related to the generation of lysosome-associated membrane protein 1 containing acidic cytoplasmic vacuoles [4,7,9,15], features found in endosomes and lysosomes. Interestingly, the vacuoles formed in response to GAELs are extremely large and visible with light microscopy (Fig. S3); thus, they are too large to be endosomes or lysosomes. Our observations suggest that these vacuoles may originate from endocytic processes as inhibition of endocytosis via temperature manipulation or with chemical inhibitors, prevent vacuolar formation and cell death [15]. While these observations intimately link endocytosis to GAEL activity, they do not reveal whether the requirement is just to transport GAELs into the cell or whether the requirement for endocytosis is related to their mechanism of cell killing or both. Ongoing studies seek to identify the pathways altered by L-Rham treatment to produce cell killing effects in HGSOC cells.

HGSOC is a genetically unstable disease [24–27] characterized by a type of genomic instability called chromosome instability (CIN) [28–32]. CIN is defined by an increase in the rate at which whole chromosomes or large parts are gained or lost [33], and is associated with intratumoral heterogeneity, poor patient outcome, and

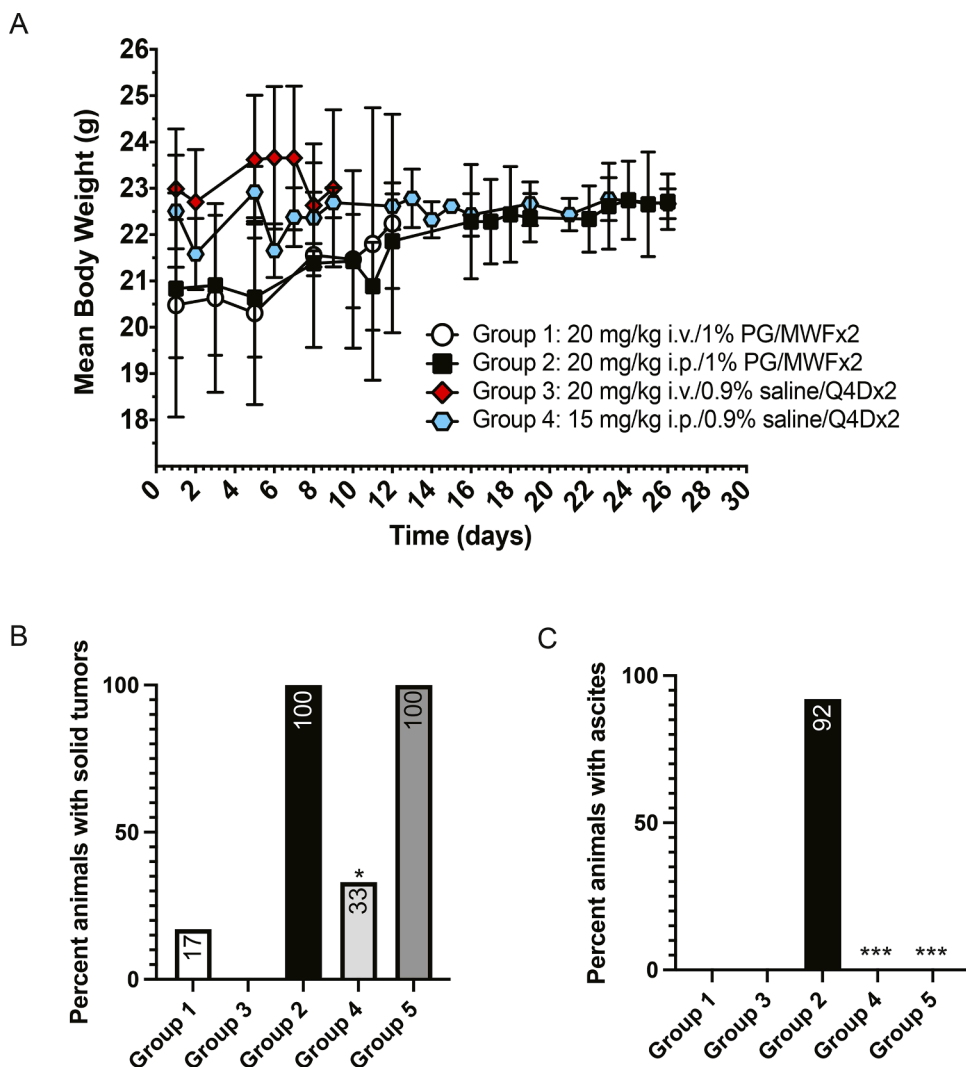


Fig. 4. Determination of maximum tolerated dose and efficacy of L-Rham in immunodeficient NRG mice. **A.** Body weight of mice after treatment with L-Rham at the indicated doses, routes, and vehicles. L-Rham was injected i.v. or i.p. on Monday/Wednesday/Friday for two weeks (M/W/Fx2), or 4 days for 4 injections (Q4Dx4), and then clinically monitored for an additional 12 days. Drugs were solubilized in either 1% propylene glycol (PG) or 0.9% saline. Bars indicate range in body weight. $N = 3$ mice per group. **B, C.** Efficacy of L-Rham on development of solid tumors (B) or ascites formation (C). Group 1 = vehicle treated (terminated day 41), Group 2 = vehicle treated (terminated day 74), Group 3 = L-Rham (terminated day 41), Group 4 = L-Rham (treatment started day 8, terminated day 74), Group 5 (treatment started day 41; terminated day 74). * or *** = significantly different from Group 2.

chemoresistance [33–38]. CIN induces changes in chromosome complements with the potential to alter large cohorts of genes (e.g., oncogenes, tumor suppressor, DNA repair genes) contributing to intratumoral heterogeneity. We demonstrated that CIN is dynamic in HGSOC patient samples throughout their course of treatment, and that CIN levels are typically higher in chemoresistant compared to chemosensitive patients [30]. The ability of L-Rham to kill patient-derived HGSOC cells was unaffected by CIN status or chemotherapy-sensitivity, suggesting GAELs may be effective agents to improve outcome in HGSOC patients.

A side-effect observed with long-term i.p. injection of L-Rham was generalized peritonitis causing adhesions of the ovary, bladder, intestines, liver, kidney, stomach, uterus to the peritoneal wall. This was not observed in NRG mice during the DRF or MTD studies. One possibility for this observation is due to puncturing of the intestinal wall during i.p. drug delivery, but it is curious that this only occurred in the L-Rham groups. Another possibility for this discrepancy is an effect of the drug with long-term exposure used for the efficacy studies (Q4Dx8; 8 treatments over 32 days) compared to the shorter duration of drug treatment in the MTD studies at Q4Dx4 (4 treatments over 16 days). Further studies will need to be conducted to determine if this is a side-effect peculiar to L-Rham, or whether this side-effect could be avoided by altering the delivery method.

The ability of L-Rham to reduce tumor burden is very promising for the treatment of HGSOC patients. L-Rham was effective when treatment

was initiated 7 days after injection of OVCAR3 cells (low tumor burden). From a modeling perspective, this is similar to initiating treatment following cytoreductive surgery. Therefore, L-Rham may be ideal in the setting of optimally debulked patients receiving adjuvant therapy, both intravenous and intraperitoneal including current regimens for Hyperthermic Intraperitoneal Chemotherapy (HIPEC) [39]. No effect on tumor mass was observed in the high tumor burden group and therefore L-Rham is unlikely to be a useful single agent for neoadjuvant chemotherapy to reduce tumor mass. It may be worthwhile to investigate a combination of L-Rham with other agents as the different mechanisms of action may synergise to effectively reduce high tumor burden. Interestingly, L-Rham blocked ascites formation, which may be beneficial for neoadjuvant, adjuvant or potentially maintenance therapy, similar to bevacizumab [40,41]. The mechanism to determine how L-Rham reduces or blocks ascites, whether as an action on tumor cells or the peritoneal vasculature, warrants further investigation.

Our previous work on EOC included assessing the *in vitro* GAEL effects on EOC cell lines and patient samples encompassing HGSOC, clear cell and endometrioid histotypes [5]. Future studies are aimed to assess the effects on poorly responsive EOCs including low grade serous and mucinous histotypes. The data showing that L-Rham as a model GAEL has *in vivo* activity is very exciting as it provides evidence that this class of drug can affect cancer burden. This holds great promise for the treatment of human cancers beyond HGSOC, since we have also shown that GAELs are effective at killing human cancer cells lines

Table 2
Summary of L-Rham efficacy on OVCAR3 i.p. xenograft in NRG mice.

Group	Group name	Dose schedule/ termination	Mice with solid tumors	Mean tumor mass (mg) ±SD ; (size range in mg)	Ascites (%)
1*	Vehicle - 1	Q4Dx8 Termination: day 41***	17% (1/6)	5 ± 0 (5)	0%
2*	Vehicle - 2	Q4Dx8 Termination: day 74***	100% (12/12)	179±102 (2–405)	92% ^{***}
3*	L-Rham - low 1	Q4Dx8 Termination: day 41***	0% (0/6)	No tumors	0%
4*	L-Rham - low 2	Q4Dx8 Termination: day 74***	33% (2/6)	332±388 (58–607)	0%
5**	L-Rham - high	Q4Dx8 Termination: day 74***	100% (6/6)	399±335 (40–777)	0%

* treatment began 7 days post OVCAR-3 cell inoculation i.p. = low tumor burden = “low”.

** treatment began 40 days post OVCAR-3 cell inoculation i.p. = high tumor burden = “high”.

*** termination of mice was 6 days post final drug administration.

^ 12 animals were used in Group 2.

~ SD = standard deviation.

*** 4/12 mice had measurable ascites (75–200 µL), 7/12 had milky or glossy ascites but there was not enough to collect.

encompassing hard to treat cancers such as pancreatic and triple negative breast cancer [6,8,19,20].

CRediT authorship contribution statement

Mark W Nachtigal: Conceptualization, Formal analysis, Funding acquisition, Investigation, Methodology, Project administration, Supervision, Validation, Writing – original draft, Writing – review & editing. **Paris Musaphir:** Formal analysis, Investigation, Methodology. **Shiv Dhiman:** Formal analysis, Investigation, Methodology. **Alon D Altman:** Formal analysis, Writing – review & editing. **Frank Schweizer:** Conceptualization, Funding acquisition, Supervision, Writing – original draft, Writing – review & editing. **Gilbert Arthur:** Conceptualization, Formal analysis, Funding acquisition, Writing – original draft, Writing – review & editing.

Declaration of Competing Interest

The authors declare no potential conflicts of interest.

Acknowledgments

We acknowledge the support of the Manitoba Tumor Bank, Winnipeg, Manitoba, that is funded by the CancerCare Manitoba Foundation and is a member of the Canadian Tissue Repository Network.

Funding

This work was supported by a University of Manitoba Bridge grant to GA, and a CancerCare Manitoba Foundation Operating grant to MWN.

Supplementary materials

Supplementary material associated with this article can be found, in the online version, at doi:10.1016/j.tranon.2021.101203.

References

- [1] C. Global Burden of Disease Cancer, C. Fitzmaurice, T.F. Akinyemiju, F.H. Al Lami, T. Alam, R. Alizadeh-Navaei, C. Allen, U. Alsharif, N. Alvis-Guzman, E. Amini, B. O. Anderson, O. Aremu, A. Artaman, S.W. Asgedom, R. Assadi, T.M. Atey, L. Avila-Burgos, A. Awasthi, H.O. Ba Saleem, A. Barac, J.R. Bennett, I.M. Bensenor, N. Bhakta, H. Brenner, L. Cahuana-Hurtado, C.A. Castaneda-Orjuela, F. Catala-Lopez, J.J. Choi, D.J. Christopher, S.C. Chung, M.P. Curado, L. Dandona, R. Dandona, J. das Neves, S. Dey, S.D. Dharmaratne, D.T. Doku, T.R. Driscoll, M. Dubey, H. Ebrahimi, D. Edessa, Z. El-Khatib, A.Y. Endries, F. Fischer, L. M. Force, K.J. Foreman, S.W. Gebrehiwot, S.V. Gopalani, G. Grosso, R. Gupta, B. Gyawali, R.R. Hamadeh, S. Hamidi, J. Harvey, H.Y. Hassen, R.J. Hay, S.I. Hay, B. Heibati, M.K. Hiluf, N. Horita, H.D. Hosgood, O.S. Ilesanmi, K. Innos, F. Islami, M.B. Jakovljevic, S.C. Johnson, J.B. Jonas, A. Kasaeian, T.D. Kassa, Y.S. Khader, E. A. Khan, G. Khan, Y.H. Khang, M.H. Khosravi, J. Khubchandani, J.A. Kopec, G. A. Kumar, M. Kutz, D.P. Lad, A. Lafranconi, Q. Lan, Y. Legesse, J. Leigh, S. Linn, R. Lunevicius, A. Majeed, R. Malekzadeh, D.C. Malta, L.G. Mantovani, B. J. McMahon, T. Meier, Y.A. Melaku, M. Melku, P. Memiah, W. Mendoza, T. J. Meretoja, H.B. Mezgebe, T.R. Miller, S. Mohammed, A.H. Mokdad, M. Moosazadeh, P. Moraga, S.M. Mousavi, V. Nangia, C.T. Nguyen, V.M. Nong, F. A. Ogbo, A.T. Olagunju, M. Pa, E.K. Park, T. Patel, D.M. Pereira, F. Pishgar, M. J. Postma, F. Pourmalek, M. Qorbani, A. Rafay, S. Rawaf, D.L. Rawaf, G. Roshandel, S. Safiri, H. Salimzadeh, J.R. Sanabria, M.M. Santric Milicevic, B. Sartorius, M. Satpathy, S.G. Sepanlou, K.A. Shackelford, M.A. Shaikh, M. Sharif-Alhoseini, J. She, M.J. Shin, I. Shiue, M.G. Shrima, A.H. Sinke, M. Sisay, A. Sligar, M.B. Sufiyani, B.L. Sykes, R. Tabares-Seisdedos, G.A. Tessema, R. Topor-Madry, T. T. Tran, B.X. Tran, K.N. Ukwaja, V.V. Vlassov, S.E. Vollset, E. Weiderpass, H. C. Williams, N.B. Yimer, N. Yonemoto, M.Z. Younis, C.J.L. Murray, M. Naghavi, Global, regional, and national cancer incidence, mortality, years of life lost, years lived with disability, and disability-adjusted life-years for 29 cancer groups, 1990 to 2016: a systematic analysis for the global burden of disease study, *JAMA Oncol.* 4 (2018) 1553–1568.
- [2] D.D. Bowtell, S. Bohm, A.A. Ahmed, P.J. Aspuria, R.C. Bast Jr., V. Beral, J.S. Berek, M.J. Birrer, S. Blagden, M.A. Bookman, J.D. Brenton, K.B. Chiappinelli, F. C. Martins, G. Coukos, R. Drapkin, R. Edmondson, C. Fotopoulou, H. Gabra, J. Galon, C. Gourley, V. Heong, D.G. Huntsman, M. Iwanicki, B.Y. Karlan, A. Kaye, E. Lengyel, D.A. Levine, K.H. Lu, I.A. McNeish, U. Menon, S.A. Narod, B.H. Nelson, K.P. Nephew, P. Pharoah, D.J. Powell, P. Ramos, I.L. Romero, C.L. Scott, A.K. Sood, E.A. Stronach, F.R. Balkwill, Rethinking ovarian cancer II: reducing mortality from high-grade serous ovarian cancer, *Nat. Rev. Cancer* 15 (2015) 668–679.
- [3] J. Prat, Ovarian carcinomas: five distinct diseases with different origins, genetic alterations, and clinicopathological features, *Virchows Arch.* 460 (2012) 237–249.
- [4] L. Jahreis, M. Renna, R. Bittman, G. Arthur, D.C. Rubinsztein, 1-O-Hexadecyl-2-O-methyl-3-O-(2'-acetamido-2'-deoxy-beta-D-glucopyranosyl)-sn-glycerol (Gln) induces cell death with more autophagosomes which is autophagy-independent, *Autophagy* 5 (2009) 835–846.
- [5] A.I. Moraya, J.L. Ali, P. Samadder, L. Liang, L.C. Morrison, T.E. Werbowetski-Ogilvie, M. Ogunsina, F. Schweizer, G. Arthur, M.W. Nachtigal, Novel glycolipid agents for killing cisplatin-resistant human epithelial ovarian cancer cells, *J. Exp. Clin. Cancer Res.* 36 (2017) 67.
- [6] M. Ogunsina, P. Samadder, T. Idowu, G. Arthur, F. Schweizer, Design, synthesis and evaluation of cytotoxic properties of bisamino glucosylated antitumor ether lipids against cancer cells and cancer stem cells, *Medchemcomm* 7 (2016) 2100–2110.
- [7] P. Samadder, R. Bittman, H.S. Byun, G. Arthur, A glycosylated antitumor ether lipid kills cells via paraptosis-like cell death, *Biochem. Cell. Biol.* 87 (2009) 401–414.
- [8] P. Samadder, Y. Xu, F. Schweizer, G. Arthur, Cytotoxic properties of D-gluco-, D-galacto- and D-manno-configured 2-amino-2-deoxy-glycerolipids against epithelial cancer cell lines and BT-474 breast cancer stem cells, *Eur. J. Med. Chem.* 78 (2014) 225–235.
- [9] G. Arthur, F. Schweizer, M. Ogunsina, Synthetic glycosylated ether glycerolipids as anticancer agents, in: J. Jiménez-Barbero, F.J. Cañada, S. Martín-Santamaría (Eds.), *Carbohydrates in Drug Design and Discovery*, Royal Society of Chemistry, Cambridge [UK], 2015.
- [10] P. Samadder, C. Richards, R. Bittman, R.P. Bhullar, G. Arthur, The antitumor ether lipid 1-Q-octadecyl-2-O-methyl-rac-glycerophosphocholine (ET-18-OCH3) inhibits the association between Ras and Raf-1, *Anticancer Res.* 23 (2003) 2291–2295.
- [11] P. Drings, I. Günther, U. Gatzmeier, F. Ulbrich, B. Khanavkar, W. Schremel, J. Lorenz, W. Brügger, H.D. Schick, J.V. Pawel, R. Nordström, Final evaluation of a phase II study on the effect of edelfosine (an Ether Lipid) in advanced non-small-cell bronchogenic carcinoma, *Onkologie* 15 (1992) 375–382.
- [12] K. Fujiwara, H. Koike, Y. Ohishi, H. Shirafuji, I. Kohn, E.J. Modest, S. Kataoka, Cytokinetic and morphologic differences in ovarian cancer cells treated with ET-18-OCH3 and the DNA-interacting agent, etoposide, *Anticancer Res.* 17 (1997) 2159–2167.
- [13] C. Gajate, F. Mollinedo, Biological activities, mechanisms of action and biomedical prospect of the antitumor ether phospholipid ET-18-OCH3 (Edelfosine), a proapoptotic agent in tumor cells, *Curr. Drug Metab.* 3 (2002) 491–525.
- [14] G. Arthur, R. Bittman, Glycosylated antitumor ether lipids: activity and mechanism of action, *Anticancer Agents Med. Chem.* 14 (2014) 592–606.
- [15] P. Samadder, H.S. Byun, R. Bittman, G. Arthur, An active endocytosis pathway is required for the cytotoxic effects of glycosylated antitumor ether lipids, *Anticancer Res.* 31 (2011) 3809–3818.

- [16] M. Ogunsina, H. Pan, P. Samadder, G. Arthur, F. Schweizer, Structure activity relationships of N-linked and diglycosylated glucosamine-based antitumor glycerolipids, *Molecules* 18 (2013) 15288–15304.
- [17] G. Yang, R.W. Franck, R. Bittman, P. Samadder, G. Arthur, Synthesis and growth inhibitory properties of glucosamine-derived glycerolipids, *Org. Lett.* 3 (2001) 197–200.
- [18] G. Yang, R.W. Franck, H.S. Byun, R. Bittman, P. Samadder, G. Arthur, Convergent C-glycolipid synthesis via the Ramberg-Bäcklund reaction: active antiproliferative glycolipids, *Org. Lett.* 1 (1999) 2149–2151.
- [19] M. Ogunsina, P. Samadder, T. Idowu, G. Arthur, F. Schweizer, Replacing D-glucosamine with its L-enantiomer in glycosylated antitumor ether lipids (GAELs) retains cytotoxic effects against epithelial cancer cells and cancer stem cells, *J. Med. Chem.* 60 (2017) 2142–2147.
- [20] M. Ogunsina, P. Samadder, T. Idowu, M.W. Nachtigal, F. Schweizer, G. Arthur, Syntheses of L-Rhamnose linked amino glycerolipids and their cytotoxic activities against human cancer cells, *Molecules* 25 (2020).
- [21] T.G. Shepherd, B.L. Theriault, E.J. Campbell, M.W. Nachtigal, Primary culture of ovarian surface epithelial cells and ascites-derived ovarian cancer cells from patients, *Nat. Protoc.* 1 (2006) 2643–2649.
- [22] P. Samadder, H.S. Byun, R. Bittman, G. Arthur, A fluorescent alkyllysophospholipid analog exhibits selective cytotoxicity against the hormone-insensitive prostate cancer cell line PC3, *Anticancer Agents Med. Chem.* 14 (2014) 528–538.
- [23] A.K. Mitra, D.A. Davis, S. Tomar, L. Roy, H. Gurler, J. Xie, D.D. Lantvit, H. Cardenas, F. Fang, Y. Liu, E. Loughran, J. Yang, M. Sharon Stack, R.E. Emerson, K.D. Cowden Dahl, M. V.B., K.P. Nephew, D. Matei, J.E. Burdette, *In vivo* tumor growth of high-grade serous ovarian cancer cell lines, *Gynecol. Oncol.* 138 (2015) 372–377.
- [24] TCGA, Integrated genomic analyses of ovarian carcinoma, *Nature* 474 (2011) 609–615.
- [25] Y.K. Wang, A. Bashashati, M.S. Anglesio, D.R. Cochrane, D.S. Grewal, G. Ha, A. McPherson, H.M. Horlings, J. Senz, L.M. Prentice, A.N. Karnezis, D. Lai, M. R. Aniba, A.W. Zhang, K. Shumansky, C. Siu, A. Wan, M.K. McConechy, H. Li-Chang, A. Tone, D. Provencher, M. de Ladurantaye, H. Fleury, A. Okamoto, S. Yanagida, N. Yanaihara, M. Saito, A.J. Mungall, R. Moore, M.A. Marra, C. B. Gilks, A.M. Mes-Masson, J.N. McAlpine, S. Aparicio, D.G. Huntsman, S.P. Shah, Genomic consequences of aberrant DNA repair mechanisms stratify ovarian cancer histotypes, *Nat. Genet.* 49 (2017) 856–865.
- [26] K.T. Kuo, B. Guan, Y. Feng, T.L. Mao, X. Chen, N. Jinawath, Y. Wang, R.J. Kurman, M. Shih Ie, T.L. Wang, Analysis of DNA copy number alterations in ovarian serous tumors identifies new molecular genetic changes in low-grade and high-grade carcinomas, *Cancer Res.* 69 (2009) 4036–4042.
- [27] K.L. Gorringe, J. George, M.S. Anglesio, M. Ramakrishna, D. Etamadmoghadam, P. Cowin, A. Sridhar, L.H. Williams, S.E. Boyle, N. Yanaihara, A. Okamoto, M. Urashima, G.K. Smyth, I.G. Campbell, D.D. Bowtell, S. Australian Ovarian Cancer, Copy number analysis identifies novel interactions between genomic loci in ovarian cancer, *PLoS ONE* 5 (2010).
- [28] M. Bungy, M.C.L. Palmer, L.M. Jeusset, N.M. Neudorf, Z. Lichtensztejn, M. W. Nachtigal, K.J. McManus, Reduced RBX1 expression induces chromosome instability and promotes cellular transformation in high-grade serous ovarian cancer precursor cells, *Cancer Lett.* 500 (2021) 194–207.
- [29] C.C. Lepage, M.C.L. Palmer, A.C. Farrell, N.M. Neudorf, Z. Lichtensztejn, M. W. Nachtigal, K.J. McManus, Reduced SKP1 and CUL1 expression underlies increases in Cyclin E1 and chromosome instability in cellular precursors of high-grade serous ovarian cancer, *Br. J. Cancer* 124 (2021) 1699–1710.
- [30] C.R. Morden, A.C. Farrell, M. Sliwowski, Z. Lichtensztejn, A.D. Altman, M. W. Nachtigal, K.J. McManus, Chromosome instability is prevalent and dynamic in high-grade serous ovarian cancer patient samples, *Gynecol. Oncol.* 161 (2021) 769–778.
- [31] L. Nelson, A. Tighe, A. Golder, S. Littler, B. Bakker, D. Moralli, S. Murtuza Baker, I. J. Donaldson, D.C.J. Spierings, R. Wardenaar, B. Neale, G.J. Burghel, B. Winter-Roach, R. Edmondson, A.R. Clamp, G.C. Jayson, S. Desai, C.M. Green, A. Hayes, F. Fojier, R.D. Morgan, S.S. Taylor, A living biobank of ovarian cancer ex vivo models reveals profound mitotic heterogeneity, *Nat. Commun.* 11 (2020) 822.
- [32] S. Penner-Goetze, Z. Lichtensztejn, M. Neufeld, J.L. Ali, A.D. Altman, M. W. Nachtigal, K.J. McManus, The temporal dynamics of chromosome instability in ovarian cancer cell lines and primary patient samples, *PLoS Genet.* 13 (2017), e1006707.
- [33] C. Lengauer, K.W. Kinzler, B. Vogelstein, Genetic instability in colorectal cancers, *Nature* 386 (1997) 623–627.
- [34] J.B. Geigl, A.C. Obenauf, T. Schwarzbraun, M.R. Speicher, Defining 'chromosomal instability', *Trends Genet.* 24 (2008) 64–69.
- [35] S.E. McClelland, Role of chromosomal instability in cancer progression, *Endocr. Relat. Cancer* 24 (2017) T23–T31.
- [36] S.E. McClelland, R.A. Burrell, C. Swanton, Chromosomal instability: a composite phenotype that influences sensitivity to chemotherapy, *Cell Cycle* 8 (2009) 3262–3266.
- [37] L.L. Thompson, L.M. Jeusset, C.C. Lepage, K.J. McManus, Evolving therapeutic strategies to exploit chromosome instability in cancer, *Cancers* 9 (2017) (Basel).
- [38] S.L. Thompson, S.F. Bakhoun, D.A. Compton, Mechanisms of chromosomal instability, *Curr. Biol.* 20 (2010) R285–R295.
- [39] W.J. van Driel, S.N. Koole, G.S. Sonke, Hyperthermic intraperitoneal chemotherapy in ovarian cancer, *N. Engl. J. Med.* 378 (2018) 1363–1364.
- [40] S. Mabuchi, Y. Terai, K. Morishige, A. Tanabe-Kimura, H. Sasaki, M. Kanemura, S. Tsunetoh, Y. Tanaka, M. Sakata, R.A. Burger, T. Kimura, M. Ohmichi, Maintenance treatment with bevacizumab prolongs survival in an *in vivo* ovarian cancer model, *Clin. Cancer Res.* 14 (2008) 7781–7789.
- [41] C.S. Walsh, Latest clinical evidence of maintenance therapy in ovarian cancer, *Curr. Opin. Obstet. Gynecol.* 32 (2020) 15–21.